ELSEVIER

Journal of Alloys and Compounds 460 (2008) 357–362

Journal of ALLOYS AND COMPOUNDS

www.elsevier.com/locate/jallcom

New lithium gas sorbent III. Experimental data on evaporation

K. Chuntonov [a,*], J. Setina [b], A. Ivanov [c], D. Permikin [c]

[a] *Nanoshell Materials R&D GmbH, Primoschgasse 3, 9020 Klagenfurt, Austria*
[b] *Institute of Metals and Technology, 1000 Ljubljana, Slovenia*
[c] *Ural State University, Lenin Avenue 51, 620083 Ekaterinburg, Russia*

Received 4 May 2007; received in revised form 14 June 2007; accepted 15 June 2007
Available online 19 June 2007

Abstract

The kinetics of lithium evaporation from Ag–Li wire has been studied experimentally in the temperature interval 520–630 °C. The initial stage of the process takes place in the kinetic regime and finishes with the formation of a thin layer of silver on the surface of the alloy. Then the process moves to the diffusion region where the evaporation flow and the mass of the deposited film can be described quantitatively with the help of simple analytical expressions.

Keywords: Lithium films; Solid solutions; Evaporation rate; Cover layer; MEMS

1. Introduction

Solid solutions of Li in Ag, Cu and some other metals are a very convenient getter material, which is easily passivated by several methods and is also easily activated by means of heating to 150–350 °C [1]. When the temperature of these alloys is raised to 450–600 °C they turn into vapor sources of Li, which condensing on the substrate, forms active getter layers characterized by high sorption activity especially with respect to oxygen and oxygen containing gases [2,3].

In this connection, it is possible to discuss two different directions in the development of getter technologies based on lithium alloys. One consists of developing vacuum pumps or gas purifiers, which use the sorption potential of heated foils or plates. The foils or plates can be produced mechanically by rolling the ingots [1]. We will discuss these issues in our next paper.

Another direction refers to the field of film technologies, when lithium or its alloy is deposited onto the set surface in the form of a getter film for maintaining vacuum inside sealed-off devices. In the first place we should mention here vacuum packed micro electro-mechanical systems (MEMS) [4–7], a rapidly developing and very specific sector of new technologies.

The presence of moving parts inside MEMS, extremely small sizes of enclosed cavities with a correspondingly high surface-to-volume ratio of cavity, as well as a long operating lifetime require a high sorption capacity of getters and the absence of loose particles [8–10]. However, it should be recognized that these requirements are mutually exclusive if one bears in mind traditional non-evaporative getters (NEGs), based on transition metals such as Ti, Zr, etc. [11–13]. Gas sorption by transition metals at room temperature continues only until the surface is saturated (one or, in the best case, several molecular layers). Therefore, though dense films of the given metals satisfy the requirement of the absence of loose particle formation, at the same time, they have a negligibly small sorption capacity. High porosity sintered materials such as high porosity thin film (HPTF) [14], the sorption capacity of which is approximately two orders of magnitude higher than that of dense films, generate free particles [15,16] due to their powder origin.

But even HPTF-getters are not able to ensure conditions necessary through the lifetime of the MEMS. A simple calculation using typical MEMS-level values shows that, e.g. to maintain a pressure of $\sim 10^{-3}$ mbar in a cavity with a volume of $\sim 1\ mm^3$ over 20 years at a standard leak rate of 10^{-10} atm cc/s, it would

* Corresponding author. Tel.: +43 650 62 03 565.
E-mail address: konstantin@chuntonov.com (K. Chuntonov).

0925-8388/$ – see front matter © 2007 Elsevier B.V. All rights reserved.
doi:10.1016/j.jallcom.2007.06.055

be necessary to use a getter with HPTF properties, which is many times larger in volume than the cavity itself.

A really high sorption capacity at room temperature can only be achieved in materials containing chemically active metals: alkalis, alkali-earths, and rare-earths. In this case, gas sorption takes place according to the known mechanism of oxidation of metals, namely, by the growth of a layer of reaction products on the metal/gas boundary [17,18]. Under vacuum conditions, when the process kinetics is small due to the negligible density of one of the components, even active metals form on their surface, not porous, but dense layers of oxides, nitrides and other compounds without loose particle formation, having a structure close monocrystalline. The sorption capacity in film getters of this nature can approach their theoretical limit that is about four orders of magnitude higher than in the case of HPTF-getters.

Of the active metals, lithium is the most suitable candidate to take the role of the main getter in MEMS technologies. Possessing the highest diffusion mobility, lithium allows maintaining the sorption kinetics at the maximum high level. Moreover, the unique ability of lithium to form solid solutions in a wide concentration range with Ag, Au, Co and Cu [19] makes it possible to overcome easily all of the technological limits connected with the chemical activity of lithium itself. Finally, alloys Ag–Li, Cu–Li, etc. due to their ductility are ideal vapor sources for thermal deposition of films of uniform thickness onto substrates of any shape. By shaping the alloy into beads, wire, or strips, it is possible to obtain evaporation flows for all types of symmetry.

However, to control the deposition processes, it is necessary to know how the rate of lithium evaporation from its solid solutions changes with temperature and time.

Previously, Ag–Li films have already been used as a reservoir for Li atoms in laser sources of lithium ions for accelerators [20–23]. The focus of these studies was on the diagnostics of lithium plasma but not on the evaporation kinetics and the changes in the film, which accompany evaporation.

The aim of the present paper is to provide concrete knowledge for the case of wire vapor sources taking into consideration the results of formal theoretical analysis of the processes taking place in the alloy itself [24]. The conclusions obtained for linear vapor sources can easily be generalized for the case of point or planar sources.

2. Experimental method

The process of Li evaporation from Ag–Li wires was studied by a rather simple but reliable method: by determination of the mass of condensate Δm_{Li} obtained by deposition during time Δt at temperature T of the wire. The mass of the lithium film was calculated from the data on the concentration of the solution formed as a result of washing the film with a known amount of pure water [3]. A Perkin-Elmer 2380 flame atomic absorption spectrometer was used for this purpose. The deviation in determination of the mass of Li did not exceed 7%.

The principal scheme of a deposition cell is given in Fig. 1. Inside a vacuum chamber, a tested wire 1 with diameter of 0.5 mm was connected vertically to two contacts Ni-conductors 4, which were strong enough for holding wire 1. A thermocouple 3 with diameter 0.1 mm was spot-welded to the lower part of the heated region 1. This installation of the wire was used for several deposition operations.

Two sets of measurements were performed using different materials and substrate sizes. In the first set of measurements, lithium deposition was performed from an Ag–28.5 at.% Li alloy onto a quartz tube 2 which was coaxial with filament 1. The tube 2 was 29 mm in diameter and 120 mm high, and provided capturing of the entire evaporation flow along the filament region of 40 mm.

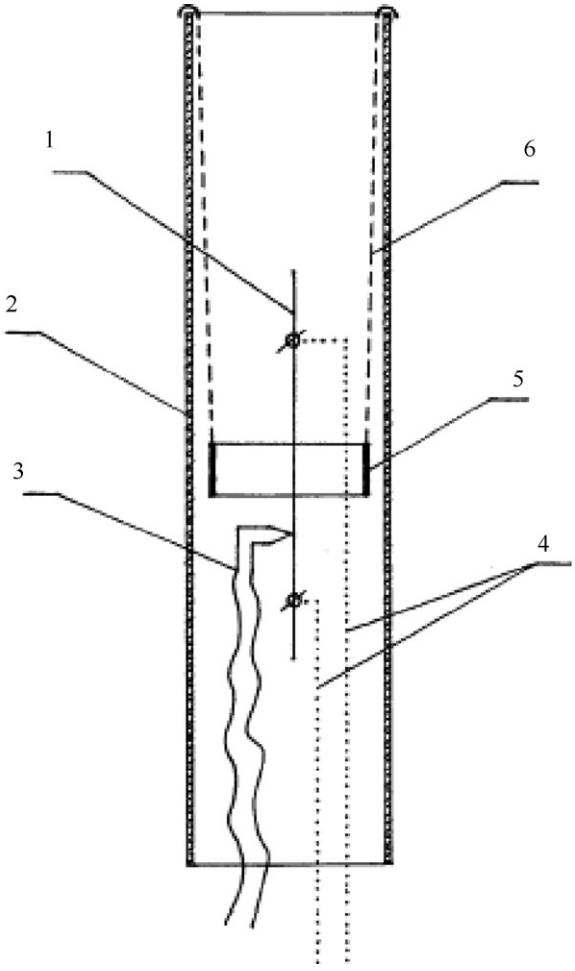

Fig. 1. Design of a deposition cell: (1) Ag–Li filament; (2) quartz tube; (3) thermocouple; (4) connecting wires; (5) steel ring; (6) string.

In the second set of measurements, an Ag–25 at.% Li alloy served as the lithium source and steel tube ring 5, fixed with the help of wire string 6 in a symmetric position with respect to 1, served as the substrate. The ring 5 was 8 mm high. The dimensional proportions of the assembly are more or less exactly shown in Fig. 1.

Both sets of measurements consisted of several single depositions, the first of which was started after a preliminary bakeout of the entire cell at 300–350 °C for about 12 h and the next one, directly after a basic pressure of 10^{-7} mbar had been achieved without heating, i.e. at room temperature. During lithium evaporation, while heating of filament 1 by current, the total pressure in the system increased approximately by one order of magnitude. After each single deposition operation, the corresponding substrate, 2 or 5, was taken out through the upper port of the vacuum chamber for chemical analysis of the condensate and replaced by a new one.

Ag–Li wire was manufactured using an ordinary wire-drawing technique from alloys obtained by melting the initial metals and further homogenizing of the mixture in evacuated steel ampoules [1]. Ag (Alfa Aesar, 99.999%) and Li (Chemetal, 99.9%) were used as the alloy components.

3. Results and discussion

Sorption studies of lithium films [3] showed that the material works most effectively when the film thickness is 120–200 Å.

Table 1
Experimental data for deposition of lithium onto a quartz substrate

No.	T (K)	Δt (s)	c_0 (at.%) Li	Δm_{Li} (mg)	$\Delta\bar{h}$ (Å)
1	793	140	28.5	0.016 ± 0.001	83
2	823	690	28.4	0.029 ± 0.002	150
3	838	505	28.3	0.040 ± 0.0025	207
4	848	600	28.2	0.055 ± 0.003	285
5	903	265	28.0	0.072 ± 0.005	373

This predetermined both the general planning and details of the present experiment.

The data for the first set of depositions (quartz substrate) are given in Table 1. Here c_0 is the gross composition of the Ag–Li wire after introduction of the correction for the loss of lithium during the previous deposition procedure, and $\Delta\bar{h}$ is the average thickness of the lithium layer on the substrate.

As can be seen, the deposition of films of thickness 100–300 Å is accompanied by a rather marginal change in the total concentration of the evaporated component. This means that a vapor source such as an Ag-Li wire allows performing multiple depositions of thin lithium layers with a practically constant rate within the bounds of a single deposition.

According to the data in Table 1, the linear rate of film growth $v = \Delta\bar{h}/\Delta t$ on the inside cylindrical surface with a diameter from 10 to 100 mm is within the range of 0.1–4.0 Å/s. At these values of v, the process of deposition of monoatomic Li-layers can be easily controlled automatically or manually.

However, the gradual decrease in the total concentration of lithium in the source leads to the monotonic decrease in the evaporation rate. To compensate for this decrease, it is necessary to raise the temperature of the wire accordingly or to increase the deposition interval Δt.

Graphs $\bar{j} - T$ in Fig. 2 give some idea of how the evaporation flow changes with temperature and time. Here curve 1 refers to the set of depositions onto the quartz substrate, curve 2 refers to the set of depositions onto the steel substrate, and $\bar{j}$ is the average evaporation rate during the time Δt. It can be seen that curve 2 is situated a little lower than curve 1, which is connected to the lower lithium content in the source in the deposition of the second set.

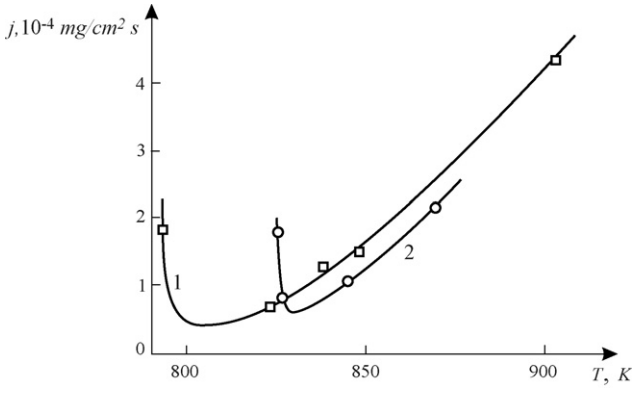

Fig. 2. Curves $\bar{j} - T$ according to the data of Table 1: (1) quartz substrate; (2) steel substrate.

At the same time, the curves are similar in shape and both are characterized by the presence of a minimum, which is considerably shifted to the initial region of each deposition set. At first sight, such a minimum seems to be an anomaly as both constituents of the evaporation process, namely, the transfer of lithium atoms into the vapor phase and the diffusion of these atoms from the volume of the wire to the surface, are increasing functions of the temperature. Meanwhile, the above-mentioned behavior of the curves $\bar{j} - T$ is to be expected, and the following two facts are important in understanding what is taking place: the implicit dependence of the $\bar{j} - T$ curves on time and the diffusionless character of evaporation in the initial stage of the process.

According to our deposition procedure, the series of experimental points that form curves 1 and 2 (Fig. 2) is an evolutionary sequence. From deposition to deposition, not only is a change in the total concentration of lithium in the wire taking place, but also the development of high chemical non-homogeneity in it. In fact, this non-homogeneity determines the value of the evaporation flow. In essence, the graphs in Fig. 2 show the function $\bar{j}(T, t)$, of which it is known that $\partial j(T, t)/\partial T > 0$, and $\partial j(T, t)/\partial t < 0$ [24]. Hence, the appearance of the minimum in curves $\bar{j}(T, t)$ is inherent in the very nature of this function.

To make it clearer, let us establish the physical meaning of the processes taking place in a wire that is periodically heated. During the first heating of the initially chemically homogeneous wire, only lithium atoms from the surface and from the borders of the surface thin layer evaporate. The evaporation rate at this stage is maximal. As a result of the loss of lithium, a thin layer which almost completely consists of atoms of the non-volatile metal, is created on the surface. That is, a diffusion barrier is formed in the material, which abruptly decreases the evaporation rate.

At the same time, raising the temperature of the source in every next deposition operation leads to the increase in evaporation flow (Fig. 2). The growth of the evaporation rate is conditioned, in particular, by the fact that for the discussed materials, the energy of the diffusion activation is higher than the energy of evaporation. So, although the thickness of the cover layer depleted in lithium increases with time, the surface lithium concentration also grows due to the temperature rise and this becomes a cause for the growth of j [24].

Thus, the unusual appearance of the experimental curves $\bar{j} - T$ is sensibly explained from the position of the theory [24] which predicts the formation of a thin film of non-volatile metal on the surface of a solid solution when its volatile component evaporates. These ideas are applied below in the derivation of a simplified method of calculation of evaporation flow in metal systems with intensive evaporation of one of the components.

4. Calculation of the evaporation flow

Let us consider the problem of evaporation of metal A from a solid solution where the second component B has vapor pressure many orders of magnitude lower than A. The vapor source consists of a wire with length l and radius r_0 and with initial concentration of volatile metal c_0. The wire is placed along an axis of an evacuated tube and heated with the current to a temperature

T, after which evaporation of A starts and the vapor condenses on the inner wall of the tube. It is required to define the evaporation rate of A from the wire and the mass of the condensate which appears on the wall during time t.

The general solution for a problem of this kind is given in [24], but now our target is to obtain a working formula for calculating a flow $j(T, t)$ taking into account the real behavior of the material, i.e. taking into account the data contained in Table 1 and Fig. 2. These data as well as the conclusions from the theoretical analysis [24] indicate that already during the first few seconds of heating, the source surface gets covered with a thin layer, which is practically deprived of the volatile component. This layer determines further process behavior.

4.1. Approximation of the cover layer

The mathematical model of the process is presented in the Appendix. In the assumed variables, the evaporation flow is equal to

$$j = hc_0 u(\tau, 1), \tag{1}$$

where $h = (RT/2\pi M)^{1/2} \exp(-E/RT)$, R is the gas constant, M the molar mass of the volatile metal, and E is the molar energy of evaporation of the same metal. For lithium alloys with Ag, Cu and some other transition metals, the mass transfer parameter $H = hr_0/D_c \gg 1$, where $D_c = D_0 \exp(-Q/RT)$, D_0 is a preexponential factor and Q is the molar activation energy of diffusion. In this case, a radial distribution of the volatile component concentration $u(\tau, x)$ is described by relation (4) as shown in the Appendix.

A graphic representation of the function $u(\tau, x)$ is given in Fig. 3. It can be seen that the core of the material is slowly involved in the process whereas the surface, on the other hand, immediately loses component A and is practically covered with a film of metal B. During evaporation under isothermal conditions,

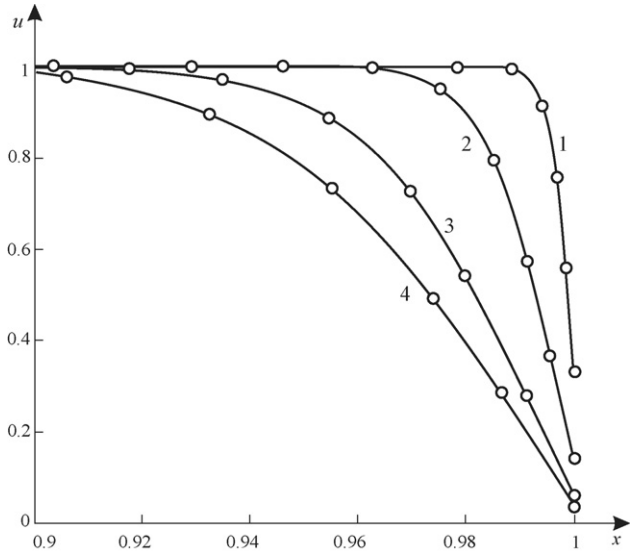

Fig. 3. Dependence of dimensionless concentration u on relative coordinate x at $H = 500$ at different moments of time τ: (1) $\tau = 10^{-5}$; (2) $\tau = 10^{-4}$; (3) $\tau = 5 \times 10^{-4}$; (4) $\tau = 10^{-3}$; lines—formula (4); circles—strict solution [24].

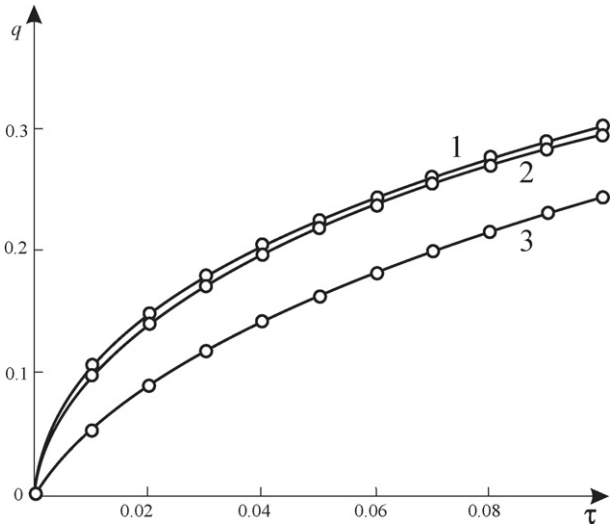

Fig. 4. Dependence of dimensionless mass q on evaporation time at different values of H: (1) $H = 1000$; (2) $H = 100$; (3) $H = 10$; lines—formula (7); circles—strict solution [24].

the outer layer B becomes thicker with time and the surface concentration $u(\tau, 1)$ of the volatile metal continues to decrease, which in accordance with (1), sets the pace of evaporation.

By substituting (4) into (1) and passing on to the dimension variables, after certain transformations, we arrive at a formula for the evaporation flow for the case of a source with a cover layer

$$j(t) \approx c_0 \left(\sqrt{\frac{D_c}{\pi t}} - \frac{D_c}{2r_0} \right). \tag{2}$$

The amount of evaporated metal is found by integrating the evaporation rate with respect to time

$$m(t) \equiv 2\pi r_0 l \frac{M}{N} \int_0^t j(t)\,\mathrm{d}t = 2\pi r_0^2 l M c_0 q \left(\frac{D_c t}{r_0^2} \right) \tag{3}$$

where c_0 is expressed in mol/m^3, N is Avogadro's constant, and for calculating $q = q(\tau)$ the model provides two possibilities (see Appendix): a rather complicated but exact eq. (7) or a simplified eq. (8). To make the choice easier in Figs. 4 and 5, the results of the calculations of the evaporated masses according to a strict solution [24] are compared with the results based on (7) and (8), respectively. It can be seen that, while approximation (7) almost exactly reproduces the data for the strict solution (Fig. 4), in the case of (8) there are certain deviations from it, which gradually grow with the decrease in the value H (Fig. 5).

4.2. Comparison with the experiment

Formula (3) allows calculating the amounts of metal deposited by a wire of known composition at a temperature T during time t. In our case, the values necessary for calculations were found from the thermodynamic properties of Ag–Li alloys [3] and by fitting of the data of Table 1. It was found that $E = 137$ kJ/mol, $Q = 220$ kJ/mol and $D_0 = 3.0$ m^2/s.

Table 2
Calculation results and experimental data for deposition of lithium films from Ag–28.5 at.% Li wire with diameter 0.5 mm

No.	T (K)	Δt (s)	D_c (m^2/s)	Δm_{Li}^{exp} (g)	Δm_{Li}^{th} (mg)	$m_{Li}^{exp}/\Delta m_{Li}^{th}$
1	793	140	1.06×10^{-14}	0.016	0.0164	0.98
2	823	690	1.4×10^{-14}	0.029	0.0292	0.99
3	838	505	5.7×10^{-14}	0.040	0.0402	1.0
4	848	600	1.16×10^{-13}	0.055	0.0553	0.99
5	903	265	5.5×10^{-13}	0.072	0.0723	1.0

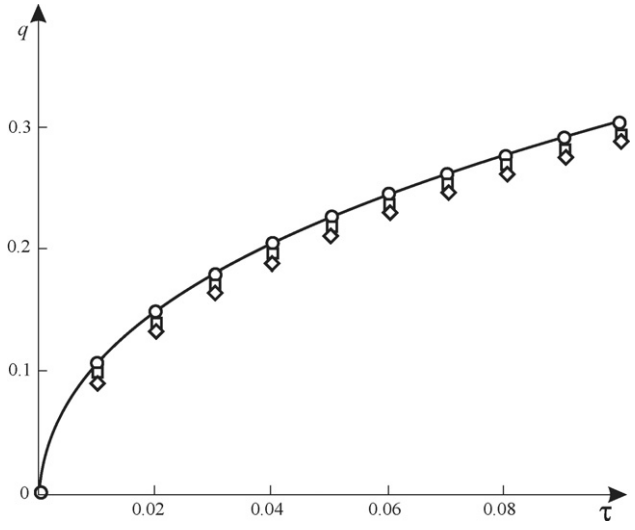

Fig. 5. Dependence of dimensionless mass q on evaporation time: line—formula (8); symbols—strict solution [24] for different values of H (circles: $H = 1000$; squares: $H = 100$; rhombs: $H = 50$).

The calculations were made for an initially homogeneous Ag–Li wire of composition $c_0 = 28.5$ at.% Li. The resulting value of lithium distribution of each preceding calculation was taken further as the initial value for the following calculation. The theoretical values of Δm_{Li}^{th} are compared with the experimental values of Δm_{Li}^{exp} in Table 2.

The presented data show that the divergence between the calculated and the observed values does not exceed 2%. Hence, eqs. (2) and (3) can be used in the practice of deposition of lithium films from solid solutions of Ag–Li, Cu–Li, etc.

5. Conclusions

1. Wires of Ag–Li alloys with lithium concentrations not higher than ~30 at.% are well-controlled and convenient direct filament lithium vapor sources in the temperature range 520–630 °C. In this range, the linear rates of Li-film growth are values of approximately 0.1–10 Å/s.
2. Experimental curves $\bar{j}(T,)$ obtained in a sequence of depositions with elevated temperature from one source have a clear minimum in the initial region of the curve, which is conditioned by a transition from a kinetic stage of evaporation to a diffusion one. This initial stage is responsible for the formation of the Ag cover layer on the source surface.
3. Simple analytical expressions have been obtained for calculation of the evaporation flow and the deposited mass (eqs. (2) and (3), respectively).

Appendix A

The mathematical model of the evaporation process is:

$$\frac{\partial c}{\partial t} = \frac{D_c}{r}\frac{\partial}{\partial r}\left(r\frac{\partial c}{\partial r}\right), \quad t > 0,\ 0 < r < r_0$$

$$c(0,\ r) = c_0$$

$$-D_c\frac{\partial c}{\partial r} = hc, \quad t > 0,\ r = r_0,$$

where r is a radial coordinate, $c(t, r)$ is the distribution of the concentration of component A at the moment of time t, D_c is the coefficient of diffusion of A in a lattice of metal B, and h is the evaporation coefficient.

Let us introduce dimensionless variables and functions: coordinate $x = r/r_0$, $0 < x < 1$; time $\tau = tD_c/r_0^2$; concentration $u = c/c_0$; mass exchange coefficient $H = hr_0/D_c$.

In the new variables, the problem has a form

$$\frac{\partial u}{\partial \tau} = \frac{1}{x}\frac{\partial}{\partial x}\left(x\frac{\partial u}{\partial x}\right), \quad \tau > 0,\ 0 < x < 1$$

$$u(0,\ x) = 1$$

$$-\frac{\partial u}{\partial x} = Hu, \quad \tau > 0,\ x = 1$$

The strict solution of the problem has a form [24]

$$c(t, r) = c_0\sum\nolimits_{k=1}^{\infty} C_k J_0\left(\frac{\lambda_k r}{r_0}\right)\exp\left(-\frac{\lambda_k^2 Dt}{r_0^2}\right),$$

$$j(t) = hc_0\sum\nolimits_{k=1}^{\infty} C_k J_0(\lambda_k)\exp\left(-\frac{\lambda_k^2 Dt}{r_0^2}\right),$$

where expansion coefficients C_k

$$C_k = \frac{\int_0^1 J_0(\lambda_k x)x\,\mathrm{d}x}{\int_0^1 J_0(\lambda_k x)^2 x\,\mathrm{d}x} = \frac{2H}{J_0(\lambda_k)(\lambda_k^2 + H^2)},$$

λ_k are eigenvalues, which are found from a solution of the transcendental equation

$$\lambda_k J_1(\lambda_k) = H\,J_0(\lambda_k), \quad k = 1, 2, 3\ldots,$$

and $J_0(z)$ and $J_1(z)$ are the Bessel zero- and first-order functions, respectively.

This solution is difficult to use due to the slow convergence of the corresponding series.

A simple approximation with acceptable accuracy for the basic function $u(\tau, x)$ can be obtained with the assumption that $H \gg 1$ and that the initial stage of evaporation takes place only with the participation of surface layers. Then for $u(\tau, x)$, we can write [24]

$$u(\tau, x) \cong 1 - \mathrm{erfc}\left(\frac{1-x}{2\sqrt{\tau}}\right)\left(1 + \frac{1}{2H}\right) + \frac{2\sqrt{\tau}}{\sqrt{\pi}(1 - x + 2H\tau)} \exp\left[-\frac{(1-x)^2}{4\tau}\right], \quad (4)$$

where erfc (z) is an additional error integral:

$$\mathrm{erfc}(z) = \frac{2}{\sqrt{\pi}} \int_z^\infty \exp(-z^2)\,\mathrm{d}z.$$

From here we come to dimensionless evaporation flow

$$y(\tau) \approx \exp(H^2\tau)\,\mathrm{erfc}(H\sqrt{\tau}) - \frac{\left[1 - \exp(H^2\tau/4)\,\mathrm{erfc}(H\sqrt{\tau}/2)\right]}{2H}, \quad H >> 1. \quad (5)$$

Eq. (5), which is exact everywhere except for a small neighborhood of point $\tau \approx 0$, can be substituted with a small sacrifice of accuracy for the asymptotic expression

$$y(\tau) \approx \frac{1}{H}\left(\frac{1}{\sqrt{\pi\tau}} - \frac{1}{2}\right), \quad (6)$$

which is a dimensionless equivalent of eq. (2). The amount of evaporated metal is found by integration of (5) with respect to time

$$q(\tau) \equiv H \int_0^\tau y(\tau)\,\mathrm{d}\tau = 2\sqrt{\frac{\tau}{\pi}} - \frac{\tau}{2} + \frac{1}{H}\left[\exp(H^2\tau)\,\mathrm{erfc}(H\sqrt{t}) - 1 + 2\sqrt{\frac{\tau}{\pi}}\right] + \frac{1}{H^2}\left[\exp\left(\frac{H^2\tau}{4}\right)\mathrm{erfc}\left(\frac{H\sqrt{\tau}}{2}\right) - 1\right]. \quad (7)$$

At very large values of H, a radical simplification of (7) is admissible

$$q(\tau) = 2\sqrt{\frac{\tau}{\pi}} - \frac{\tau}{2}. \quad (8)$$

References

[1] K. Chuntonov, G. Voronin, O. Malyshev, EP1791152 (November 29, 2005).
[2] J.A. Rodriguez, J. Hrbek, J. Phys. Chem. 98 (1994) 4061.
[3] K. Chuntonov, J. Setina, J. Alloys Compd. 455 (2008) 489.
[4] B. Stark (Ed.), MEMS Reliability Assurance Guidelines for Space Application, JPL Publication 99-1, Pasadena, CA, 1999.
[5] K. Gilleo, MEMS packaging issues and materials, in: Proceeding of 33rd International Symposium on Microelectronics (IMAPS), Boston, MA, September 20-22, 2000, pp. 598–604.
[6] D. Sparks, J. Trevino, S. Massoud-Ansari, N. Najafi, J. Micromech. Microeng. 16 (2006) 2488.
[7] S.J. Randolph, M.D. Hale, M.A. Guillorn, P.D. Rack, M.L. Simpson, Microelectron. Eng. 77 (2005) 412.
[8] B. Lee, S. Seok, K. Chun, J. Micromech. Microeng. 13 (2003) 663.
[9] H. L. Curtis, M. C. Glenn, J. B. DCamp, L. A. Dunaway, US Patent Appl. 20,040,183,177 (Sept. 23, 2004).
[10] D. Sparks, S. Massoud-Ansari, N. Najafi, J. Micromech. Microeng. 15 (2005) 1560.
[11] E. Giorgi, B. Ferrario, IEEE Trans. Electron Dev. 36 (1989) 2744.
[12] C. Benvenuti, P. Chiggiato, P. Costa Pinto, A. Escudeiro Santana, T. Hedley, A. Mongelluzzo, V. Ruzinov, I. Wevers, Vacuum 60 (2001) 57.
[13] Brochure SAES Getters: PaGe^{TM} Films, 2005.
[14] Brochure SAES Getters: FED HPTF Getter, 2004.
[15] D. Sparks, S. Massoud-Ansari, N. Najafi, IEEE Trans. Adv. Packaging 26 (2003) 277.
[16] K. Chuntonov, H. Ipser, K. Richter, EP 060 02762.0 (10 February, 2006).
[17] K. Hauffe, Reaktionen in und an Festen Stoffen, Springer-Verlag, Berlin, 1955.
[18] O. Kubaschewski, B.E. Hopkins, Oxidation of Metals and Alloys, Butterworths, London, 1967.
[19] H. Okamoto, Phase Diagrams for Binary Alloys, ASM International, Materials Park, OH, 2000.
[20] P.L. Dreike, G.C. Tisone, J. Appl. Phys. 59 (1986) 371.
[21] G.C. Tisone, K.W. Bieg, P.L. Dreike, Rev. Sci. Instrum. 61 (1990) 562.
[22] T.J. Renk, G.C. Tisone, R.G. Adams, D.J. Johnson, C.L. Ruiz, G.W. Cooper, Phys. Plasmas 6 (1999) 3697.
[23] B. Gerber, M. Lopez, K. Lamppa, W. Stearns, K. Bieg, In Situ Evaporation of Lithium for LEVIS Ion Source, Technical Report SAND-93-2183, Sandia National Labs, Albuquerque, NM, 1994.
[24] K. Chuntonov, A. Ivanov, D. Permikin, J. Alloys Compd. 456 (2008) 187.